ELSEVIER

International Journal of Pharmaceutics 126 (1995) 199–208

international journal of pharmaceutics

Dissolution kinetics and solubilities of *p*-aminosalicylic acid and its salts

R.T. Forbes[a], P. York[a,*], J.R. Davidson[b]

[a] *Postgraduate Studies in Pharmaceutical Technology, the School of Pharmacy, University of Bradford, Bradford, BD7 1DP, UK*
[b] *Pfizer Central Research Ltd., Sandwich, Kent, CT13 9NJ, UK*

Received 17 February 1995; revised 8 May 1995; accepted 1 June 1995

Abstract

A series of metal and amine salts of *p*-aminosalicylic acid (PAS) were synthesized and their water solubilities and intrinsic dissolution rates investigated. Whilst the increased solubility of PAS in the presence of its major breakdown product *m*-aminophenol (MAP) dictated that equilibrium solubilities were unable to be determined, apparent solubilities at 10°C after 1 h equilibration were obtained. The order of decreasing solubility and intrinsic dissolution rate for metallic salts of PAS was potassium > sodium > calcium (low hydrate) > calcium (trihydrate) = magnesium. When data for PAS and its ammonium and ethanolamine salts were included, a direct relationship between log solubility (C_s) and log dissolution rate (IDR) was observed. Since the apparent solubility of the potassium salt was only qualitatively known, by applying this solubility-dissolution rate relationship its solubility was predicted to be 2.5 M/l^{-1} at 10°C using the regression line $\log IDR = 1.06 \log C_s - 0.166$ ($r = 0.9931$, $n = 7$). The relationship could not be used where a phase change at the solid-liquid interface occurred. Thus, the solubilities of the tosylate, mesylate and sulphate salts of PAS could not be estimated since these salts reverted during dissolution to form PAS.

Keywords: Preformulation; Salt selection; Apparent solubility; Dissolution kinetics; Metal and amine salts; *p*-Aminosalicylic acid

1. Introduction

A newly identified pharmacologically active chemical entity rarely possesses physicochemical and mechanical properties which are ideally suitable for the purposes of formulation and administration to the patient. For a candidate drug having ionizable groupings, salt formation can be a means of altering, and of potentially optimizing, these properties. In particular, drug solubility, dissolution rate and stability can be modified by the selection of different salt forms. The process of selecting an appropriate salt is therefore an essential part of the preformulation stage of drug development. However, despite the common use and importance of salts, little work has been

* Corresponding author. Tel: +44 1274 384738; Fax: +44 1274 384769.

SSDI 0378-5173(95)04126-U

performed to develop relationships that predict the effect of salt formation on the properties of a parent molecule (Gould, 1986). This situation exists partly because time and substance constraints rarely allow pharmaceutical companies the luxury of manufacturing a large range of salts for evaluation. The tuberculostatic agent *p*-aminosalicylic acid (PAS) is one example of the many drugs which have been marketed as salts. In this work a series of its salts was synthesized and their solubilities and dissolution properties evaluated, in an attempt to provide predictive information to aid the salt selection process.

Drugs of low aqueous solubility can present absorption and bioavailability problems. In such cases salt formation is often used to increase solubility and therefore a determination of the pH-solubility profile of a weak electrolyte and its salts is an important prerequisite when predicting possible dissolution problems and selecting an appropriate pharmaceutical salt. The need to consider alternative salt forms to improve solubility is primarily assessed from the equilibrium solubility of the parent molecule. Since PAS degrades in solution (Jivani and Stella, 1985), an accurate determination of its equilibrium aqueous solubility is compromised, and thus a comparison of the apparent solubilities of PAS and its salts was undertaken. A direct relationship between solubility and intrinsic rates of dissolution of various substances has been reported (Hamlin et al., 1965; Nicklasson et al., 1981) and used to estimate solubilities where limited amounts of material were available, and to aid salt selection (Nicklasson and Nyqvist, 1983). We report the use of this relationship to rank solubility in a series of salts where equilibrium solubility assessment is compromised due to decomposition in aqueous solution. In addition to the comparison of dissolution characteristics and solubility properties of PAS and its salts, relations with the nature of the counterion are explored.

2. Materials and methods

2.1. Materials

p-Aminosalicylic acid (BN: 17F-0614), potassium aminosalicylate (BN: 18F-7751) and sodium aminosalicylate dihydrate (BN: 66F-0732) all from Sigma Chemical Co., Poole, were >99% pure by TLC on manufacturer's certificate of analysis. The less than 250 micron sieve fraction was used unless otherwise stated, and the materials were coded PAS, K and NA, respectively. PAS and NA were used in the synthesis of all other salts. Other solvents and reagents were of reagent or analar grade. Water was double distilled from an all glass still and deionized.

2.2. Preparation of salts

2.2.1. General procedure

Salts of PAS were prepared either by metathetical reaction with the sodium salt or by direct reaction with PAS in a suitable solvent. Salts were recrystallized to improve purity where necessary and the resulting crystals were washed and dried. Samples were stored in sealed amber glass jars and the <250 micron sieve fraction was used for studies unless otherwise indicated.

2.2.2. Preparation of magnesium salt (batch MG)

A solution of 96 g magnesium chloride hexahydrate in 100 ml water was slowly added with stirring to a solution of 200 g NA in 250 ml warm water. Stirring was continued for 3 h, then the crystals were filtered and washed with small quantities of water. The crystals were dried at 40°C for 64 h under reduced pressure. 140 g of MG was recovered representing a yield of 74%.

2.2.3. Preparation of calcium salt hydrate (batches CA and CA2)

A solution of 38 g calcium chloride dihydrate dissolved in 50 ml of water was slowly added with stirring to a solution of 100 g NA in 140 ml of warm water. Stirring was continued for 1 h with the mixture placed in a water bath maintained at 20°C. The precipitated first crop (batch CA2), after washing with water and methanol, gave 45 g (yield 50%) and was less pure than the second crop (batch CA) obtained from the mother liquor after storage at 4°C for 5 days. The latter was washed with water and dried under reduced pressure at room temperature.

2.2.4. Preparation of calcium salt (batch CA3)

A solution of 75 g calcium chloride dihydrate dissolved in 75 ml of water was slowly added with stirring to a solution of 200 g NA in 250 ml of warm water. Stirring was continued for 2 h and the solution allowed to cool under ambient conditions. The precipitate was filtered, washed (two 25-ml portions of water) and dried at 35°C under reduced pressure overnight to give 123 g (yield 75%).

2.2.5. Preparation of ammonium salt (batch NH4)

Ammonia solution 35% (33 ml) was slowly added with stirring to a suspension of 100 g PAS in 350 ml ethanol 96%. The mixture was heated until complete solution had occurred and then allowed to cool for 2 h with stirring. The crystals were filtered, washed (two 20-ml portions of ethanol) and dried at 40°C under reduced pressure overnight to give 32.9 g (yield 30%).

2.2.6. Preparation of ethanolamine salt (batch ETH)

Ethanolamine (40 ml) was slowly added with stirring to a suspension of 100 g PAS in 350 ml ethanol 96%. The mixture was heated until complete solution had occurred and then allowed to cool for 2 h with stirring. The crystals were filtered, washed (two 30-ml portions of ethanol) and dried at 40°C under reduced pressure overnight to give 104 g (yield 74%).

2.2.7. Preparation of hydrochloride salt (batch HCl)

Molar hydrochloric acid (700 ml) was slowly added with stirring to a solution of 100 g PAS in 800 ml acetone. Stirring was continued for 2 h and the resulting fine white precipitate was then filtered, washed (three 150-ml acetone/water 1:1 portions) and dried at 40°C under reduced pressure overnight to give 85 g (yield 68%).

2.2.8. Preparation of sulphate salt (batch SO4)

Concentrated sulphuric acid (9 ml) was slowly added with stirring to a solution of 50 g PAS in 500 ml acetone. Stirring was continued for 30 min and the resulting fine white precipitate was then filtered, washed with acetone and dried at 35°C under reduced pressure overnight to give 65 g (yield 99%).

2.2.9. Preparation of mesylate salt (batch MES)

Methanesulphonic acid (45 ml) was slowly added with stirring to a solution of 100 g PAS in 800 ml acetone. Stirring was continued for 30 min and the resulting fine white precipitate was then filtered, washed (two 100-ml acetone portions) and dried at 40°C under reduced pressure overnight to give 158 g (yield 97%).

2.2.10. Preparation of tosylate salt (batch TOS)

A solution of 125 g of *p*-toluenesulphonic acid dissolved in 500 ml acetone was slowly added with stirring to a solution of 100 g PAS in 1000 ml acetone. Stirring was continued for 1 h and the resulting fine white precipitate was then filtered, washed (three 150-ml acetone portions) and dried at 40°C under reduced pressure overnight to give 163 g (yield 73%).

2.2.11. Confirmation of salt synthesis

Elemental analysis (Control Equipment Corporation, Model 240HX) and water content (by method of Karl Fischer titration) were determined. The formulae of the prepared salts are given in Table 1 and results of elemental analysis are presented in Table 2. Further confirmatory evidence of salt synthesis was provided from DSC, NMR, UV and IR data.

2.3. Differential scanning calorimetry (DSC)

Scans were recorded on a Perkin-Elmer DSC7 differential scanning calorimeter connected to a Perkin-Elmer 7700 computer via the TAC7 microprocessor controller. Samples were scanned in sealed aluminium volatile sample pans at a heating rate of 10°C/min with nitrogen as the purge gas and indium as the calorimetric standard.

2.4. X-ray powder diffraction (XRPD)

X-ray powder diffraction patterns were recorded using a Siemens, Model D500 diffrac-

Table 1
Formulae of PAS and its prepared salts

Sample	Structure of salt counterion	Molecular formula
PAS		$C_7H_7NO_3$
K	K^+	$C_7H_6NO_3$
NA	Na^+	$NaC_7H_6NO_3 \cdot 2H_2O$
MG	Mg^{++}	$Mg(C_7H_6NO_3)_2 \cdot 4H_2O$
CA	Ca^{++}	$Ca(C_7H_6NO_3)_2 \cdot 3H_2O$
CA2	Ca^{++}	$Ca(C_7H_6NO_3)_2 \cdot 3H_2O$
CA3	Ca^{++}	$Ca(C_7H_6NO_3)_2 \cdot O \cdot 8H_2O$
NH4	NH_4^+	$C_7H_{10}N_2O_3$
ETH	$(OH)CH_2CH_2NH_3^+$	$C_9H_{14}N_2O_4$
HCl	Cl^-	$C_7H_8NO_3Cl$
SO4	SO_4^{2-}	$(C_7H_8NO_3)_2SO_4$
TOS	$CH_3C_6H_4SO_3^-$	$C_{14}H_{15}NO_6S$
MES	$CH_3SO_3^-$	$C_8H_{11}NO_6S$

tometer fitted with a scintillation counter and a CuKα radiation source. Discs from the intrinsic dissolution studies were blotted dry and allowed to air dry at room temperature before being fixed to standard perspex holders. Data were collected between 3 and 73° 2θ in a step scan mode with a step size of 0.02° 2θ and a collecting time of 1 s/step.

2.5. Solubility determinations

2.5.1. Determination of apparent aqueous solubilities of PAS and its salts

Apparent solubilities were determined after 1 h equilibration in water at a temperature of 10 ($\pm$0.5)°C using a shaking water bath and cooler (Grant, Cambridge). Screw-capped amber glass vials containing 10 ml of water were positioned in the water bath and brought to equilibrium temperature. Two-gram samples were then added to the vials and experiments were carried out at least in duplicate. No attempt was made to determine solubilities in excess of 200 mg/ml. After 1 h, samples were filtered through 0.45 μm pore size

Table 2
Elemental analyses of PAS salts

Sample		Analysis % w/w				
		C	H	N	M[a]	H_2O
MG	Calc.	41.97	5.03	6.99	6.07	18.0
	Found	(42.14)	(5.07)	(6.97)	nd	(18.6)
CA	Calc.	42.21	4.55	7.03	10.06	13.6
	Found	(42.47)	(4.47)	(6.90)	(10.1)	(12.8)
CA2[b]	Calc.	42.21	4.55	7.03	10.06	13.6
	Found	(40.49)	(4.44)	(6.48)	(9.7)	(13.0)
CA3	Calc.	46.86	3.82	7.80	nd	4.0
	Found	(46.46)	(3.68)	(7.61)	nd	(3.7)
NH4	Calc.	49.41	5.92	16.46	nd	nd
	Found	(49.11)	(5.89)	(16.33)	nd	nd
ETH	Calc.	50.46	6.59	13.08	nd	nd
	Found	(50.25)	(6.66)	(12.85)	nd	nd
HCl	Calc.	44.34	4.25	7.39	nd	nd
	Found	(44.28)	(4.26)	(7.27)	nd	nd
SO4	Calc.	41.59	3.99	6.93	nd	nd
	Found	(41.24)	(4.01)	(6.87)	nd	nd
TOS	Calc.	51.69	4.65	4.31	nd	nd
	Found	(51.46)	(4.61)	(4.28)	nd	nd
MES	Calc.	38.55	4.45	5.62	nd	nd
	Found	(38.59)	(4.46)	(5.53)	nd	nd

[a]Metal ion.
[b]Sample does not meet purity criteria of $\pm$0.4% C, H, N.

Millipore filters. One millilitre of each filtrate was appropriately diluted with mixed phosphate buffer pH 6.8, BP, and analysed by UV spectrophotometry at 300 nm. The pH values (Orion research Model 811) of the filtrates were recorded.

2.5.2. Determination of apparent pH-solubility profile

The apparent solubility of PAS was determined at various solution pH values. The pH of 0.5 M potassium chloride solution was adjusted by the addition of standard HCl and NaOH solutions. An excess of PAS was added to 50 ml of solution in a screw-capped 120 ml amber glass vial. After 2 h equilibration using a shaking water bath maintained at 25°C the concentration of PAS was determined by UV spectrophotometry as above. The pH of the filtrate was determined (Orion Research Model 811) and measurements were made in triplicate at each pH.

2.6. Intrinsic dissolution rate (IDR)

Intrinsic dissolution rates were determined employing a static-disc modified USP XXI paddle method (USP apparatus No. 2) using a precalibrated dissolution bath (G.B. Caleva, Model 7ST) at various rotation speeds and temperatures.

Each sample (300 $\pm$ 5 mg) was compressed in a 13 mm infrared punch and die set to 705 MNm^{-2} (10 tons) for approximately 1 min. The metal surfaces in contact with the drug were prelubricated using a 5% w/v solution of stearic acid in chloroform. The compressed disc was then placed centrally at the bottom of a stainless steel cylinder of dimensions 20 × 25 mm internal diameter. Molten paraffin wax was used to hold the disc in position and allowed to solidify. The exposed face of the disc was scraped carefully to remove any residual wax and transferred lubricant.

The disc in its holder was positioned centrally at the bottom of the dissolution vessel containing 900 ml of pre-equilibrated dissolution medium and a paddle (USP apparatus No. 2) rapidly lowered to a position 10 mm above the surface of the disc holder. Rotation at a fixed speed was then commenced. The dissolution medium was recirculated by a Model 202U peristaltic pump (Watson Marlow, Falmouth) through 0.1 mm flow cells. The amount of drug appearing in the dissolution medium with time was determined by UV spectrophotometry (Hewlett Packard Model HP8451A diode array spectrophotometer) at an analytical wavelength of 300 nm using previously determined absorption coefficients. Intrinsic dissolution rates were calculated from the slopes of the concentration-time plots by linear regression analysis and were determined in triplicate.

3. Results and discussion

3.1. Solubility studies

Initial experiments revealed that aqueous equilibrium PAS solubility could not be determined using UV analysis. This was because the UV absorbance continued to increase with time and did not reach equilibrium. The additive contribution to absorbance at 300 nm from increasing amounts of the degradation product *m*-aminophenol (MAP) was thought to be responsible.

HPLC was therefore used to discriminate between MAP and PAS concentrations. However, the concentration of PAS did not remain constant and showed a continued increase. A plot of PAS concentration against MAP concentration at a given time gave a linear relation. This indicated that the solubility of PAS is dependent on MAP concentration and that MAP acts to 'salt in' PAS in a similar manner to that reported by Müller et al. (1977) and to that shown by Carstensen and Attarchi (1988) for aspirin and salicylic acid.

Unable to determine equilibrium solubilities, Hou and Poole (1969) and later Tsuji et al. (1978) determined 'apparent solubility' values after 2 h equilibration and at various pH, for ampicillin and related aqueous unstable amphoteric penicillins. In the present study determination of the apparent solubility of PAS before 2 h equilibration was appropriate, since preliminary studies showed that the concentration of MAP was low and not significant at this time.

The apparent solubilities of PAS and its salts are presented in Fig. 1. The values obtained are

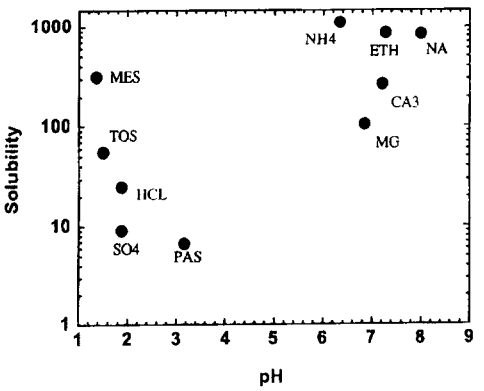

Fig. 1. Relation between apparent solubilities at 10°C (expressed as M/l PAS content $\times 10^3$) and filtered solution pH of PAS and its salts.

generally in accordance with ionic equilibria considerations and pH-solubility theory. Salt formation with either basic or acidic counterions gave the increased solubility expected for an amphoteric molecule such as PAS and resulted in the U-shaped pH-solubility profile. K was highly soluble (>200 mg/ml) and therefore an accurate value was not determined. Salts of the carboxylic acid group were generally more soluble than salts of the basic amine group. This finding is in line with the relative acidity and basicity of the carboxylic acid (pK_a 3.6) and amine (pK_a 1.8) groups, PAS being very weakly basic. On examining the data for the salts of the acid group, the divalent salts MG and CA were less soluble than monovalent salts NA, ETH and NH4. Chowhan (1978) and Anderson and Conradi (1985) observed similar results finding that solubility decreased with charge on the cation.

The general shape of the PAS pH-solubility profile (Fig. 2) was comparable with that composed of individual salt data (Fig. 1). However, the differences in solubility of the salts did not appear to be solely due to a pH effect and thus compromised a possible simple predictive relationship. In particular the ammonium-based salts ETH and NH4 were more soluble than metallic salts of PAS at similar pH. Pandit et al. (1989) also observed an increased solubility for an ethanolamine salt over inorganic cation salts. These salts of PAS may have an increased solubility due to the ammonium-based counterions exerting a hydrotropic and a structuring effect upon water molecules.

When the rank solubility order for metallic PAS salts is compared with rank order data for other carboxylic acids (Chowhan, 1978; Anderson and Conradi, 1985), a general trend of salts of divalent cations being less soluble than salts of monovalent cations is apparent. A more precise general prediction of the effect of salt species on the solubility of organic carboxylic acids is not possible. A possible explanation may be found in that in the PAS series the solubility of the calcium salt depended on its degree of hydration; the solubility of the trihydrate CA2 was lower than the less hydrated CA3. When comparing the rank orders obtained for the various carboxylic acids, the different degrees of hydration of the salts may have acted to modify solubility such that no consistent solubility order for the different salt series was observed. This explanation is further supported from the work of Rubino (1989) who observed that the log solubilities of a series of sodium salts were inversely related to both the melting point and stoichiometric amounts of water in the crystal hydrates.

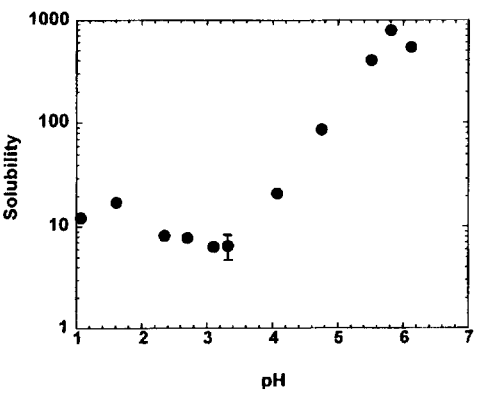

Fig. 2. Apparent pH-solubility profile for PAS in water at 25°C after 2 h equilibration (solubility expressed as M/l PAS content $\times 10^3$). (Error bars denote S.D. and can be within data point.)

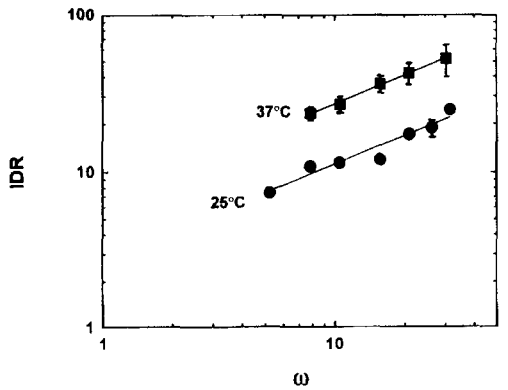

Fig. 3. Variation of intrinsic dissolution rate (IDR, M/cm^2 per s × 10^6,) of PAS into aqueous solution with stirrer angular velocity (ω, rad/s). (Error bars denote S.D.)

3.2. Dissolution kinetics of PAS

The effect of hydrodynamic conditions on dissolution rate was used to determine the process controlling the rate of dissolution. Under sink conditions for diffusion from a disk source the rate of dissolution, J, is given by the Levitch (1962) equation:

$$J = 0.62AD^{2/3}\upsilon^{-1/6}\omega^{1/2}C_s \quad (1)$$

where A, D, and C_s are the surface area, diffusion coefficient and solubility respectively, υ is the kinematic viscosity and ω is the angular velocity of rotation. From Eq. (1) since J is proportional to $\omega^{0.5}$ then IDR $= J/A$ may be expressed as:

$$\text{IDR} = a\omega^{0.5} \quad (2)$$

where a is a constant. From Eq. (2) a plot of log IDR versus log ω will have a slope of 0.5 for diffusion controlled dissolution under laminar flow conditions.

Intrinsic dissolution rates for PAS into aqueous solutions at 25 and 37°C were determined at various paddle rotation speeds. Fig. 3 shows the log-log plots of IDR versus ω obtained for PAS at 25 and 37°C. An increase in the paddle speed ω gave rise to an increase in IDR according to Eq. (2). Both plots are linear and slopes of 0.59 and 0.61 were calculated for the two temperatures, respectively, confirming that dissolution was essentially diffusion controlled. Turbulence was indicated to play some part in controlling dissolution since both slopes have values greater than 0.5.

The temperature dependence of the intrinsic dissolution rate of PAS was investigated. Nicklasson et al., 1988 determined the activation energy (E_a) for the dissolution process of the organophosphorus poisoning antidote HI-6 by linear regression analysis from Arrhenius plots. The activation energy of PAS was likewise determined. Intrinsic dissolution rates for PAS into aqueous solution at various temperatures (10–37°C) were determined at a paddle rotation speed of 100 rev./min. Fig. 4 shows an Arrhenius plot of the dissolution rate of PAS in water (100 rev./min). A correlation coefficient of 0.9986 was obtained by linear regression analysis ($n = 4$) and the activation energy (E_a) for the dissolution process was calculated to be 41.0 kJ/mole. The enthalpy of activation for the dissolution process at 25°C (ΔH^*) was calculated according to Eq. (3):

$$E_a = \Delta H^* + RT \quad (3)$$

where $R = 8.314$ J/mol K^{-1} and T is the temperature, K. A value of 38.5 kJ/mole was obtained for E_a.

Whilst recognizing that only four data points are available, a linear relationship is indicated in

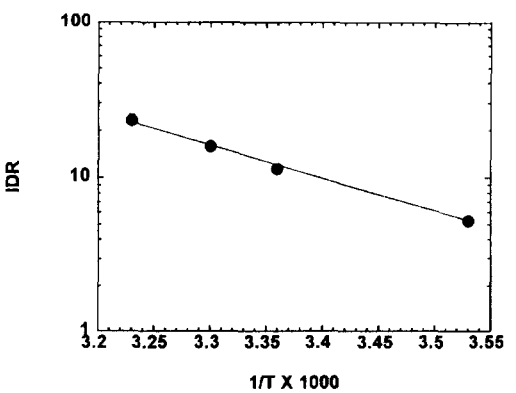

Fig. 4. Variation of intrinsic dissolution rate (IDR, M/cm^2 per s × 10^6) of PAS into aqueous solution with inverse temperature (K^{-1}) using a stirrer speed of 100 rev./min. (Error bars denote S.D.)

Fig. 4 demonstrating that the PAS solid phase underwent no transformation over the temperature range investigated. The activation energy of 41.0 kJ/mole for the dissolution process is similar to that reported for amoxicillin trihydrate at 38.0 kJ/mole (Tsuji et al., 1978). The solubility of amoxicillin is quoted as 0.013 M/l at 25°C and very similar to that of PAS, thus data for the two chemical forms show good agreement. The enthalpy of dissolution, ΔH^*, of PAS was 38.5 kJ/mole at 25°C. This high value is consistent with the low solubility of PAS and indicates that the energy difference between solid and liquid phase is relatively high. For other poorly soluble compounds, e.g. sulphamethizole, ΔH^* values of around 40–50 kJ/mole are reported (Nicklasson et al., 1982). For freely soluble bacampicillin hydrochloride a much reduced value of 17 kJ/mole is reported (Nicklasson et al., 1988). Although the conditions and hydrodynamics of the dissolution processes for the materials studied differed between these reports, the values of ΔH^* are qualitatively comparable and possibly useful in ranking solubility.

3.3. Comparison of aqueous IDR of PAS and its salts

From Eq. (1) a direct relationship between solubility and dissolution rate exists which has been confirmed experimentally (Hamlin et al., 1965). Because of solution instability it was not possible to determine equilibrium solubilities of PAS and its salts and therefore the use of IDR was investigated as a means of ranking their solubilities. Under the time course of the dissolution experiment the degradation of PAS and its salts in solution was negligible. This is because dissolution kinetics can be obtained within minutes, whereas equilibrium solubility measurements are frequently obtained after days.

Intrinsic dissolution rates for PAS and its salts into aqueous solution at 10°C were determined at a paddle rotation speed of 100 rev./min. Linear plots were obtained for most samples when cumulative amounts of each salt (expressed as mg PAS per 900 ml) dissolved were plotted with time and indicated that the Noyes-Whitney equation was applicable. Intrinsic dissolution rates are presented as a histogram in Fig. 5. Similar trends to those observed for apparent solubilities of the salts were observed in that the IDR of salt forms was greater than that of PAS. Salts of the carboxylic acid gave greater rates than salts of the amine group. The order of decreasing solubility for metallic salts of PAS was K > NA > CA3 > CA2 = MG. This same order was observed for the intrinsic dissolution rates of the salts. When PAS, ETH and NH4 were also included a direct relationship between log solubility and log dissolution rate was obtained.

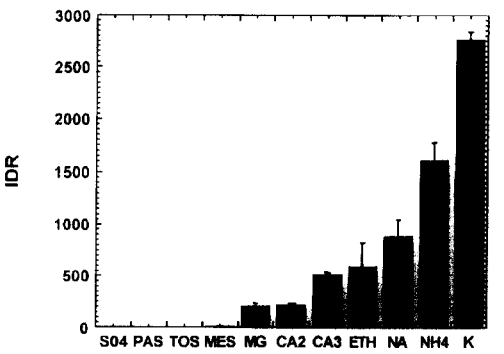

Fig. 5. Intrinsic dissolution rates (IDR, M/cm^2 per s × 1000, expressed as PAS equivalent) of PAS and its salts into water at a temperature of 10°C and using a stirrer speed of 100 rev./min. (Error bars denote S.D.)

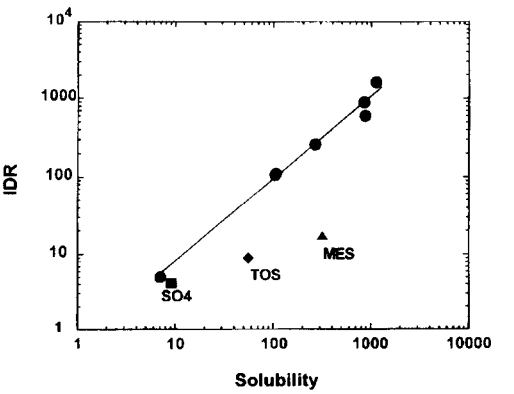

Fig. 6. Relation between intrinsic dissolution rate (IDR, M/cm^2 per s × 10^6,) and apparent solubility (S, M/l × 10^3) of PAS and its salts in water at 10°C.

Fig. 6 shows the log-log plot of dissolution rate against apparent solubility for PAS and its salts. From the Noyes-Whitney equation, such a plot should give a slope of unity. Nicklasson et al. (1981) obtained a slope of 1.02 using different compounds to those we report here. In our work a slope of 1.06 was obtained for the least squares line of best fit, for seven of the PAS salts. The other three salts, SO4, TOS, MES deviated from this line. In an attempt to investigate this deviation X-ray powder diffractometry and DSC were performed on the post-dissolution, dried disc surfaces. Differences in the X-ray diffractograms were observed for each of the three salts when comparing data obtained before and after dissolution, that indicated the formation of PAS at the solid surface. Further evidence of a conversion to PAS was obtained from DSC studies. The DSC scan of MES before dissolution gives a melting endotherm with a peak at 190°C. The DSC scan of MES from the disc surface after dissolution has an endotherm peaking at 143°C and is very similar to the DSC melting endotherm of PAS at 145°C. Thus DSC and XRPD data indicated that SO4, MES and TOS were unstable in their aqueous saturated diffusion layers and that PAS precipitated at the solid-liquid interface and resulted in the deviation of these salts from the linear relation. This example serves to highlight the usefulness of complementary solid-state analysis of the phase undergoing dissolution, as an aid to the interpretation of dissolution results. The poor reproducibility of data for ETH with its poorer regression coefficient may have also been due in part to a phase transition. Anderson and Conradi (1985) warned that precipitation of the free acid is more likely to be observed in salts of weak acids with conjugate weak bases, as is the case with ETH.

From Fig. 6 the linear relation obtained for a log-log plot indicates that the use of IDR to rank solubilities is valid providing the dissolving species does not undergo any phase transformation. This relationship was used to estimate K solubility from its dissolution rate. A predicted solubility of K as 2.5 M/l was obtained using the regression line $\log \text{IDR} = 1.06 \log C_s - 0.166$ ($r = 0.9931$, $n = 7$).

Table 3
Intrinsic dissolution rates (IDR, M/cm^2 per s $\times$ 10^6, expressed as PAS equivalent) of PAS and its salts into various dissolution media at a temperature of 25°C and using a stirrer speed of 100 rev./min (parentheses denote S.D.)

Dissolution medium	Sample	IDR	r	n
Water	PAS	11.4 (0.39)	0.9999	3
	TOS	18.9 (2.35)	0.9964	3
	MG	699 (0.85)	0.9990	2
0.05 M HCl	PAS	32.1 (3.85)	0.9993	3
	TOS	57.0 (4.11)	0.9981	2
	CA2	125 (15.9)	0.9991	3
	MG	177 (22.0)	0.9994	3
	NA	1019 (227)	0.9897	3
Phosphate buffer pH 6.8	PAS	107 (24.8)	0.9987	3
	TOS	30.1 (4.25)	0.9926	3

3.4. Influence of dissolution medium on IDR of PAS and its salts

The absorption of weak electrolytes from the GI tract is influenced by the regional differences in pH which affect dissolution and solubility. The influence of dissolution medium on IDR was therefore investigated to assess likely in vivo behaviour.

Approximate gastric and intestinal pH environments were simulated using 0.05 M HCl and mixed phosphate buffer pH 6.8, BP. Intrinsic dissolution rates for PAS and its salts into these media and into aqueous solution at 25°C were determined at a paddle rotation speed of 100 rev./min.

The effect of change in dissolution medium on the IDR of PAS and its salts is shown in Table 3 and was found to mirror its effect on PAS solubility. The rate of dissolution for PAS into the various media increased in the order: water < 0.05 M HCl < buffer pH 6.8, ionization of PAS in the acid and buffer favouring increased dissolution. For TOS the order was water < buffer pH 6.8 < 0.05 M HCl. Reversion of salt form to PAS in water and a self-buffering effect in buffer would act to reduce dissolution and possibly explain the observed order. For MG the dissolution rate was reduced on change of media from water to 0.05 M HCl. In the acid medium the self-

buffering effect of MG at the dissolving surface would be reduced.

A change of salt form also had an affect on dissolution rate since for each dissolution medium the dissolution rates of PAS and its salts differed. Although bulk pH may have been constant for each salt system under study, the salts exert a self-buffering action to give different pH values at the dissolving surface in the diffusion layer. For example, Serajuddin and Jarowski (1985) showed that the microenvironmental pH at the solid-liquid interface is important for controlling dissolution. They obtained good conformity of their dissolution data with the Noyes-Whitney equation when the saturated solubility in the diffusion layer is used rather than the solubility at the bulk solution pH. The solubility in the diffusion layer is estimated using the pH value of a saturated solution in the bulk pH dissolution media. Therefore, in the present study, differences in the self-buffering capacity of the salts, producing their different diffusion layer pH values, may serve to partly explain their different dissolution rates.

Acknowledgements

The authors would like to thank SERC and Pfizer Central Research (UK) for a CASE award for R. Forbes, and Mr. R. Nettleton for XRPD data collection.

References

Anderson, B.D. and Conradi, R.A., Predictive relationships in the water solubility of salts of a nonsteroidal anti-inflammatory drug. *J. Pharm. Sci.*, 74 (1985) 815–820.

Carstensen, J.T. and Attarchi, F., Decomposition of aspirin in the solid state in the presence of limited amounts of moisture II: kinetics and salting-in of aspirin in aqueous acetic acid solutions. *J. Pharm. Sci.*, 77 (1988) 314–317.

Chowhan, Z.T., pH-solubility profiles of organic carboxylic acids and their salts. *J. Pharm. Sci.*, 67 (1978) 1257–1260.

Gould, P.L., Salt selection for basic drugs. *Int. J. Pharm.*, 33 (1986) 201–217.

Hamlin, W.E., Northam, J.I. and Wagner, J.G., Relationship between in vitro dissolution rates and solubilities of numerous compounds representative of various chemical species. *J. Pharm. Sci.*, 54 (1965) 1651–1653.

Hou, J.P. and Poole, J.W., The amino acid nature of ampicillin and related penicillins. *J. Pharm. Sci.*, 58 (1969) 1510–1515.

Jivani, S.G. and Stella, V.J., Mechanism of decarboxylation of *p*-aminosalicylic acid. *J. Pharm. Sci.*, 74 (1985) 1274–1282.

Levitch, V.G., *Physicochemical Hydrodynamics*, Prentice-Hall, Englewood Cliffs, NJ, 1962 pp. 1–80.

Müller, F., Süverkrüp, R. and Ullmann, E., Die zersetzung von *p*-aminosalicylsäure in gegenwart begrenzter wassermengen *Pharm. Ind.*, 39 (1977) 1115–1122.

Nicklasson, M. and Nyqvist, H., Studies on the relationship between intrinsic dissolution rates and rates of water adsorption. *Acta Pharm. Suec.*, 20 (1983) 321–330.

Nicklasson, M., Brodin, A. and Nyqvist, H., Studies on the relationship between solubility and intrinsic rate of dissolution as a function of pH. *Acta Pharm. Suec.*, 18 (1981) 119–128.

Nicklasson, M., Brodin, A. and Stenlander, C., The dependence of intrinsic rates of dissolution on hydrodynamic conditions using a thermodynamic approach. *Acta Pharm. Suec.*, 19 (1982) 25–32.

Nicklasson, M., Fyhr, P., Magnusson, A.B. and Gunnvald, K., A preformulation study on the in vitro dissolution characteristics of the organophosphorus poisoning antidote HI-6. *Int. J. Pharm.*, 46 (1988) 247–254.

Pandit, N.K., Strykowski, J.M. and Shtohryn, L., The effect of salts on the distribution and solubility of an acidic drug *Int. J. Pharm.*, 50 (1989) 7–13.

Rubino, J.T., Solubilities and solid state properties of the sodium salts of drugs *J. Pharm. Sci.*, 78 (1989) 485–489.

Serajuddin, A.T.M. and Jarowski, C.I., Effect of diffusion layer pH and solubility on the dissolution rate of pharmaceutical acids and their sodium salts. II: Salicylic acid, theophylline, and benzoic acid. *J. Pharm. Sci.*, 74 (1985) 148–154.

Tsuji, A., Nakashima, E., Hamano, S. and Yamana, T., Physicochemical properties of amphoteric β-lactam antibiotics. I: Stability, solubility and dissolution behaviour of amino penicillins as a function of pH. *J. Pharm. Sci.*, 67 (1978) 1059–1066.